Article

Higher-Order Dispersive and Nonlinearity Modulations on the Propagating Optical Solitary Breather and Super Huge Waves

H. G. Abdelwahed [1,2,*], A. F. Alsarhana [1], E. K. El-Shewy [2,3] and Mahmoud A. E. Abdelrahman [4,5]

1   Department of Physics, College of Science and Humanities, Prince Sattam bin Abdulaziz University, Al- Kharj 11942, Saudi Arabia
2   Theoretical Physics Group, Faculty of Science, Mansoura University, Mansoura 35516, Egypt
3   Department of Physics, College of Science, Taibah University, Al-Madinah Al-Munawarah 41411, Saudi Arabia
4   Department of Mathematics, College of Science, Taibah University, Al-Madinah Al-Munawarah 41411, Saudi Arabia
5   Department of Mathematics, Faculty of Science, Mansoura University, Mansoura 35516, Egypt
*   Correspondence: h.abdelwahed@psau.edu.sa or hgomaa_eg@mans.edu.eg

Abstract: The nonlinearity form of the Schrödinger equation (NLSE) gives a sterling account for energy and solitary transmission properties in modern communications with optical-fiber energreinforcement actions. The solitary representation during fiber transmissions was regulated by NLSE coefficients such as nonlinear Kerr, evolutions, and dispersions, which controlled the energy changes through the model. Sometimes, the energy values predicted from the NLSEs computations may diverge due to variations in the amplitude and width caused by scattering, dispersive, and dissipative features of fiber materials. Higher-order nonlinear Schrödinger equations (HONLSEs) should be explored to alleviate these implications in energy and wave features. The unified solver approach is employed in this work to evaluate the HONLSEs. Steepness, HO dispersions, and nonlinearity self-frequency influences have been taken into consideration. The energy and solitary features were altered by higher-order actions. The unified solver approach is employed in this work to reform the HONLSE solutions and its energy properties. The steepness, HO dispersions, and nonlinearity self-frequency influences have been taken into consideration. The energy and soliton features in the investigated model were altered by the higher-order impacts. Furthermore, the new HONLSE solutions explain a wide range of important complex phenomena in wave energy and its applications.

Keywords: higher-order nonlinear Schrödinger equations; optical super soliton; huge waves; super huge structure

1. Introduction

Various forms of Schrödinger equations have found widespread application in applied science, energy and its implementations, particularly in performing natures in dispersive systems of shock dispersive hydrodynamic waves [1], B-Einstein condensate [2,3], and waveguide and optical solitons [4]. In many nonlinear circumstances, such as semiconductors, deep ocean, optics, plasmas flow and condensation of Bose–Einstein, the nonlinearly Schrödinger equation (NLSE) has developed into the intrinsic illustrative technique for representing wave patterns [5–7]. The majority of researchers concur that solitonic motion, or the study of self-modes trapped in most natural nonlinear environmental configurations, is a hugely important phenomenon that recurrently explains the progression of waves in a broad diversity of scientific optical, plasma, fluid, and energy applications [8–11]. By using Maxwell equations that related the light magnetic and electric fields, light propagation may be mathematically and accurately explained. The equation governing pulse propagation in optical fibers may be obtained by combining the equations for the magnetic and electric fields and performing certain mathematical computations [12]. The NLSE is important

for depicting the wave patterns of dynamical propagation modes in implementations of fiber optics

$$\psi_z - i\beta_1\psi_{tt} - i\beta_2 \mid \psi \mid^2 \psi = 0,\tag{1}$$

where ψ is the varying slow field, z (t) is the spatial (temporal) coordinate, and β_1 (β_2) is real parameter for chromatic dispersion (nonlinear Kerr) coefficient. Solitons are waves that maintain their shape when propagated at constant speed under balancing effects between dispersion and nonlinearity. The NLSE offers a phase of self-modulation effects as well as dispersion characteristics in Kerr impact applications in optical fiber experiments [13–15]. The propagating bright or dark envelopes in optical fibers are related to the balance between self-phase modulations and group velocity dispersives effects [16–18].

The NLSE ignores nonlinear effects aside from the intensity dependence of the refractive index, neglects linear loss, and approximate dispersion using the leading group velocity dispersion component. Physically, some terms must be added to incorporate what is not represented, depending on the circumstances and/or the desired precision of the computed results. This results in a generalized NLSE [19,20]. Due to the dissipative and dispersive effects on fiber composites, the predicted soliton energies are different from that discovered with NLSE. This means that HO modulations of these consequences on NLSE should be considered [5,21]. The form (1) with HO coefficients is modified in the form [5,21]:

$$\psi_z - i\beta_1\psi_{tt} - i\beta_2 \mid \psi \mid^2 \psi - \beta_3\psi_{ttt} - \beta_4(\mid \psi \mid \psi)_t - \beta_5 \mid \psi^2 \mid_t \ \psi = 0,\tag{2}$$

where β_2, β_3 are the firs- order dispersion and nonlinearity coefficients, respectively. Additionally, the higher orders of dispersive-nonlinear coefficients are β_4 and β_5. When there are higher orders of Kerr effects present, solitary optical propagations are characterized by the HOLSE with the disturbance of higher orders. The passing light intensity depends on its refractive index in the configuration of nonlinear Kerr's effects [22,23]. Numerous domains of technology and research, including applied mathematics, hydrodynamics, nuclear physics, telecommunications, transmission lines, ocean waves, and energy applications, have recently been affected by recent studies on nonlinear higher-order dynamical systems with distinct resulting behaviors [24,25].

On the other hand, in the nonlinear systems, the breathers and hybrid freak solutions have been actually researched [26–31]. It has been shown that the breather phase changes and hybrid waveform interactions rely on the physical parameters of the model equation. It has been shown how nonlinearly stimulated Raman scattering is described by the dynamical interactions and collisions of huge wave properties [32]. It was discovered that the bright, kinks, and W formal solutions are some of the self-similar solitary wave types. Solitons have received a lot of interest recently due to their robust nature and essential responsibilities in the physics of nonlinear applications [33–38].

In the ongoing work, we introduce some new solutions for HONLSE, utilizing the unified solver technique [39] to modulate the obtained structures as rational bright, rapid amplitudes and periodic waves via the introduction of higher-order effects. It has been carefully considered how these results' properties depend on and are sensitive to higher-order coefficients. It has been noted that HO coefficients dominate not only the width, amplitude, and energy of new wave excitations, but also the kind and frequency.

This study is organized as follows: Section 2 shows an intriguing equation that aggregates physical correlations between the dispersion, higher-order NLSE physical coefficients, and the transformation parameters. We also introduce some vital solutions for Equation (2). The physical interpretation of the provided answers shown in Section 3 represents the physical interpretation of the presented results. Finally, the article is concluded in Section 4.

2. Optical Solitary Solution

Utilizing the wave transformation,

$$\psi(t,z) = \Psi(\zeta) \, e^{i(cz-vt)}, \quad \zeta = t - \mu z + \zeta_0,\tag{3}$$

c, v, μ and ζ_0 are arbitrary constants.

Putting Equation (3) into Equation (2), one obtains the nonlinear equation:

$$\beta_3 \Psi''' + (2\beta_1 v - 3\beta_3 v^2 + \mu)\Psi' + (3\beta_4 + 2\beta_5)\Psi^2\Psi' + i((\beta_1 - 3\beta_3 v)\Psi'' + (\beta_3 v^3 - \beta_1 v^2 - c)\Psi + (\beta_2 - \beta_4 v)\Psi^3) = 0. \tag{4}$$

Equation (4) contains real and imaginary parts. By separate real and imaginary components, the first real part reads

$$\beta_3 \Psi''' + (2\beta_1 v - 3\beta_3 v^2 + \mu)\Psi' + (3\beta_4 + 2\beta_5)\Psi^2\Psi' = 0 \tag{5}$$

and the other imaginary, part given by

$$(\beta_1 - 3\beta_3 v)\Psi'' + (\beta_3 v^3 - \beta_1 v^2 - c)\Psi + (\beta_2 - \beta_4 v)\Psi^3 = 0. \tag{6}$$

Integrating Equation (5) and using Equation (6) via some algebraic steps, the two Equations (5) and (6) reduce to

$$\Lambda_1 \Psi'' + \Lambda_2 \Psi^3 + \Lambda_3 \Psi = 0 \tag{7}$$

and the constrain conditions

$$\mu = \frac{-\beta_3\, c - 8\beta_3^2 v^3 + 8\beta_1\beta_3 v^2 - 2\beta_1^2 v}{\beta_1 - 3\beta_3 v}, \tag{8}$$

$$\beta_5 = \frac{3(\beta_2\beta_3 - \beta_1\beta_4 + 2\beta_4\beta_3 v)}{2(\beta_1 - 3\beta_3 v)} \tag{9}$$

with

$$\Lambda_1 = 1, \quad \Lambda_2 = \frac{\beta_2 - \beta_4 v}{\beta_1 - 3\beta_3 v}, \quad \Lambda_3 = \frac{c + v^2(\beta_1 - \beta_3 v)}{3\beta_3 v - \beta_1}, \tag{10}$$

where Λ_1, Λ_2, and Λ_3 represent the physical coefficients for the lowest- and higher-order effects.

In view of the proposed solver [39], the solutions to Equation (2) are:

Family 1:

$$\Psi_{1,2}(t,z) = \pm\sqrt{\frac{6(3v^2\beta_3 - 2\beta_1 v - \mu)}{3\beta_4 + 2\beta_5}} \operatorname{sech}\left(\pm\sqrt{\frac{3v^2\beta_3 - 2\beta_1 v - \mu}{\beta_3}}(t - \mu z + \zeta_0)\right). \tag{11}$$

Thus, the solutions to Equation (2) are

$$\psi_{1,2}(t,z) = \pm\sqrt{\frac{6(3v^2\beta_3 - 2\beta_1 v - \mu)}{3\beta_4 + 2\beta_5}} \operatorname{sech}\left(\pm\sqrt{\frac{3v^2\beta_3 - 2\beta_1 v - \mu}{\beta_3}}(t - \mu z + \zeta_0)\right) e^{i(cz - vt)}. \tag{12}$$

Family 2:

$$\Psi_{3,4}(t,z) = \pm\sqrt{\frac{35(3v^2\beta_3 - 2\beta_1 v - \mu)}{6(3\beta_4 + 2\beta_5)}} \operatorname{sech}^2\left(\pm\sqrt{\frac{5\,(3v^2\beta_3 - 2\beta_1 v - \mu)}{12\beta_3}}(t - \mu z + \zeta_0)\right). \tag{13}$$

Thus, the solutions to Equation (2) are

$$\psi_{3,4}(t,z) = \pm\sqrt{\frac{35(3v^2\beta_3 - 2\beta_1 v - \mu)}{6(3\beta_4 + 2\beta_5)}} \operatorname{sech}^2\left(\pm\sqrt{\frac{5\,(3v^2\beta_3 - 2\beta_1 v - \mu)}{12\beta_3}}(t - \mu z + \zeta_0)\right) e^{i(cz - vt)}. \tag{14}$$

Family 3:

$$\Psi_{5,6}(t,z) = \pm\sqrt{\frac{3(3v^2\beta_3 - 2\beta_1 v - \mu)}{3\beta_4 + 2\beta_5}} \tanh\left(\pm\sqrt{\frac{2\beta_1 v - 3v^2\beta_3 + \mu}{2\beta_3}}(t - \mu z + \zeta_0)\right). \tag{15}$$

Thus, the solutions to Equation (2) are

$$\psi_{5,6}(t,z) = \pm\sqrt{\frac{3(3v^2\beta_3 - 2\beta_1 v - \mu)}{3\beta_4 + 2\beta_5}}\, \tanh\left(\pm\sqrt{\frac{2\beta_1 v - 3v^2\beta_3 + \mu}{2\beta_3}}\,(t - \mu z + \zeta_0)\right)e^{i(cz-vt)}. \tag{16}$$

3. Results and Discussion

In several domains, Equation (2) has been solved using a variety of numerical and analytical approaches. To obtain an exact solitary solution for our model, Equation (6) can be integrated and transformed into a dynamical energy equation in the form:

$$\frac{1}{2}\Psi'(\zeta)^2 = -\frac{2(c + v^2(\beta_1 - \beta_3 v))}{12\beta_3 v - 4\beta_1}\Psi(\zeta)^2 + \frac{(\beta_2 - \beta_4 v)}{12\beta_3 v - 4\beta_1}\Psi(\zeta)^4. \tag{17}$$

By solving Equation (17), the exact solution can be obtained in the form:

$$\begin{aligned}
\Psi(z,t) \;=\; & 2\sqrt{2}\Big(c + v^2(\beta_1 - \beta_3 v)\Big)\sqrt{\frac{(\beta_1 - 3\beta_3 v)^2}{(\beta_2 - \beta_4 v)(c + v^2(\beta_1 - \beta_3 v))}} \\[4pt]
& \exp\!\Big(\sqrt{\frac{c + v^2(\beta_1 - \beta_3 v)}{\beta_1 - 3\beta_3 v}}\,(\zeta_0 + t - \mu z) + i(c\,z - tv)\Big) \\[4pt]
& \big((\beta_1 - 3\beta_3 v)(\exp(2\sqrt{\tfrac{c + v^2(\beta_1 - \beta_3 v)}{\beta_1 - 3\beta_3 v}}\,(\zeta_0 + t - \mu z)) + 1)\big).
\end{aligned} \tag{18}$$

This solution produces very stable breather envelopes and soliton waves as depicted in Figures 1 and 2. Furthermore, the suggested solver produces several solutions (12), (14), (16), the physical nature of which mostly depends on the coefficients for lowest (higher) order effects. Many solution forms are obtained by the solver method such as breather envelopes and solitons, as shown in Figures 3 and 4 in addition to periodic rational and explosive blow up as per Figures 5 and 6.

On the other hand, the positive and negative values of $\beta_1\beta_2$ demonstrate the solution type desired for modulation stability for creating waves structure as dark, bright, and huge forms. The modulations of field form in slow-amplitude variations can produce randomly external perturbation forms of dark and bright envelopes as per [40,41]:

$$\psi(t,z) = \Lambda e^{i(c\,z - tv)}\tanh\left(\frac{\zeta_0 + t - \mu z}{\sqrt{2}\sqrt{\left|\frac{\beta_1}{\beta_2\Lambda}\right|}}\right) \tag{19}$$

and

$$\psi(t,z) = \Lambda e^{i(c\,z - tv)}\operatorname{sech}^2\left(\frac{\zeta_0 + t - \mu z}{\sqrt{2}\sqrt{\left|\frac{\beta_1}{\beta_2\Lambda}\right|}}\right). \tag{20}$$

Furthermore, to obtain freak wave solutions, the rational huge self-focusing solutions of the first-second types have been given as [42]

$$\Psi_1(z,t) = \sqrt{2}\sqrt{\frac{\beta_1}{\beta_2}}\,e^{2i\beta_1 z}\left(-1 + \frac{4 + 16i\beta_1 z}{4t^2 + 16\beta_1^2 z^2 + 1}\right), \tag{21}$$

and

$$
\begin{aligned}
\Psi_2(z,t) \;=\; & \sqrt{\frac{\beta_1}{\beta_2}}\,e^{2i\beta_1 z}\Big(1 + \big(-\frac{t^4}{2} - 6\beta_1^2 t^2 z^2 - \frac{3t^2}{2} - i\beta_1 z(t^4 + 4\beta_1^2 t^2 z^2 - 3t^2 + \\
& 4\beta_1^4 z^4 - 2\beta_1^2 z^2 - \frac{15}{4}) - 10\beta_1^4 z^4 - 9\beta_1^2 z^2 + \frac{3}{8}\big)/\big(\frac{t^6}{12} + \frac{1}{2}\beta_1^2 t^4 z^2 + \\
& \frac{t^4}{8} + \beta_1^4 t^2 z^4 - \frac{3}{2}\beta_1^2 t^2 z^2 + \frac{9t^2}{16} + \frac{2}{3}\beta_1^6 z^6 + \frac{9}{2}\beta_1^4 z^4 + \frac{33}{8}\beta_1^2 z^2 + \frac{3}{32}\big)\Big).
\end{aligned}
\tag{22}
$$

The propagation of envelope dark and bright waves are illustrated in Figures 7 and 8. The physical effects of coefficients β_1 and β_2 on the structure properties of these waves are given in Figures 9–12. It was noted that β_1 increases the width of dark and solitonic waves, while β_2 decreases the the width of dark and solitonic waves as depicted in Figures 9–12. In another ward, the existence of first to second freak waves in this model are shown in Figures 13 and 14. Furthermore, Figures 15 and 16 illustrate how variables β_1 physically change the structural characteristics of huge waveforms. It was discovered that β_1 raises the first huge and second super freak amplitudes as in Figures 15 and 16.

Finally, the higher-order combined dispersion and dissipation effects in coefficients β_3 and β_4 are reported in Figures 17–20. It is noted that β_3 increases both the amplitude and width of the solver solution (14), while β_4 dominated the amplitude and width of the same solution as in Figures 17–20. In summary, a unified solver has investigated the characteristics of higher-order solutions of breather envelopes, dark, bright, huge, rational, explosive, and solitons in addition to enhance the wave representation of novel structures as super freaks.
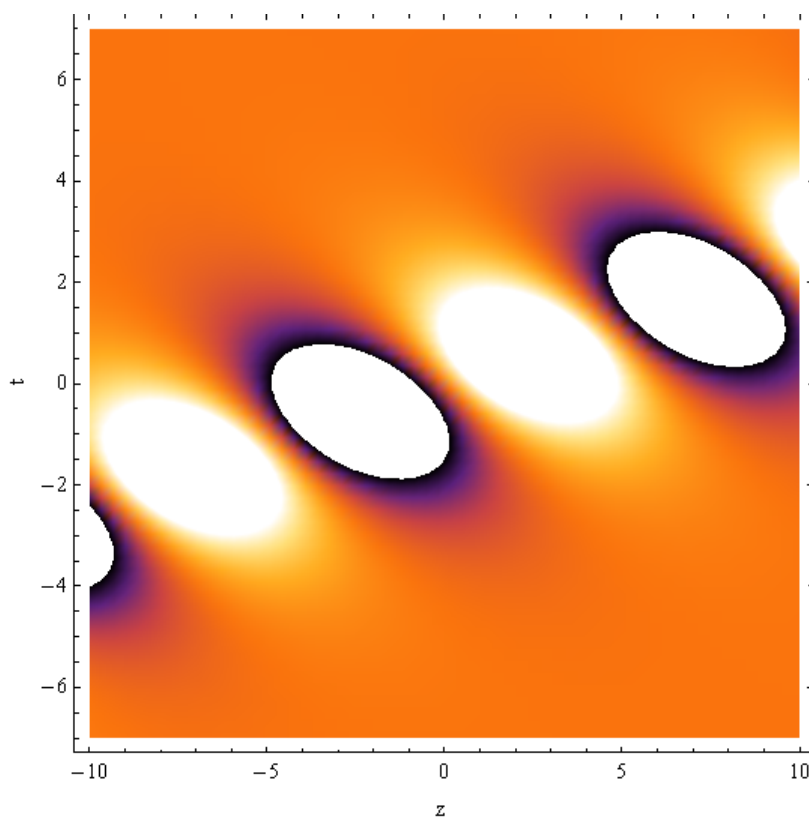

Figure 1. Change of real part of solution (18) with z, t for $c = 0.5, v = 0.7, \beta_1 = 0.1, \beta_2 = 1, \beta_1 = 0.1, \beta_3 = 0.3, \beta_4 = 0.2$.
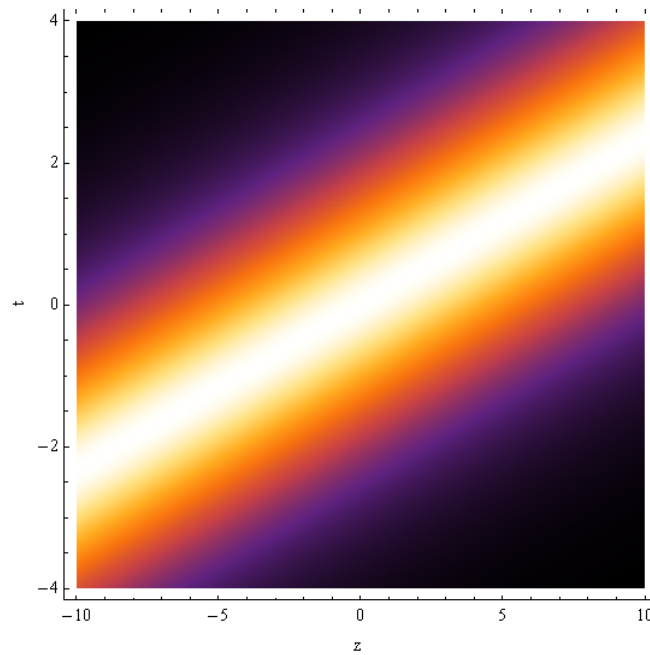
Figure 2. Change of absolute value of solution (18) with z, t for $c = 0.5$, $v = 0.7$, $\beta_1 = 0.1$, $\beta_2 = 1$, $\beta_1 = 0.1$, $\beta_3 = 0.3$, $\beta_4 = 0.2$.
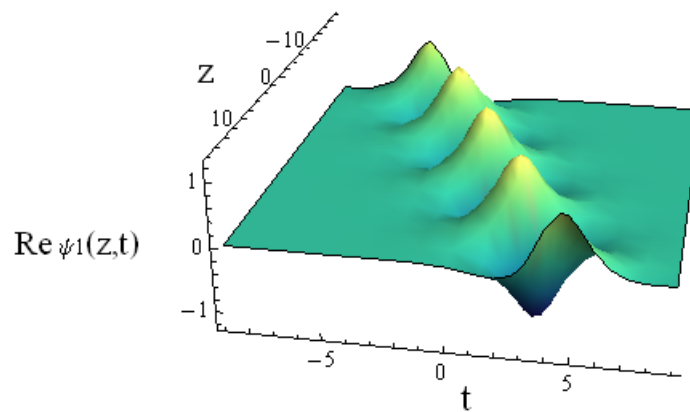

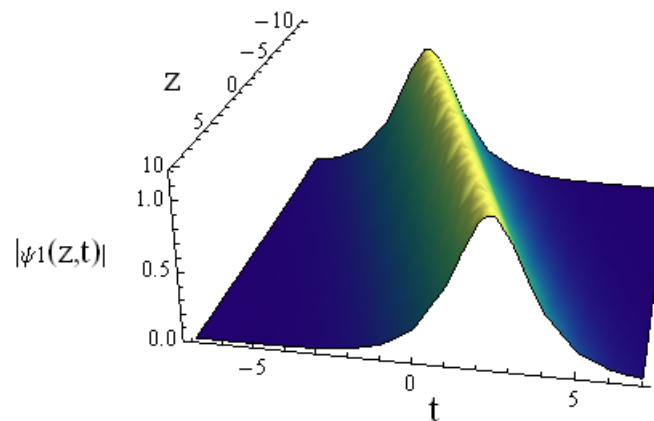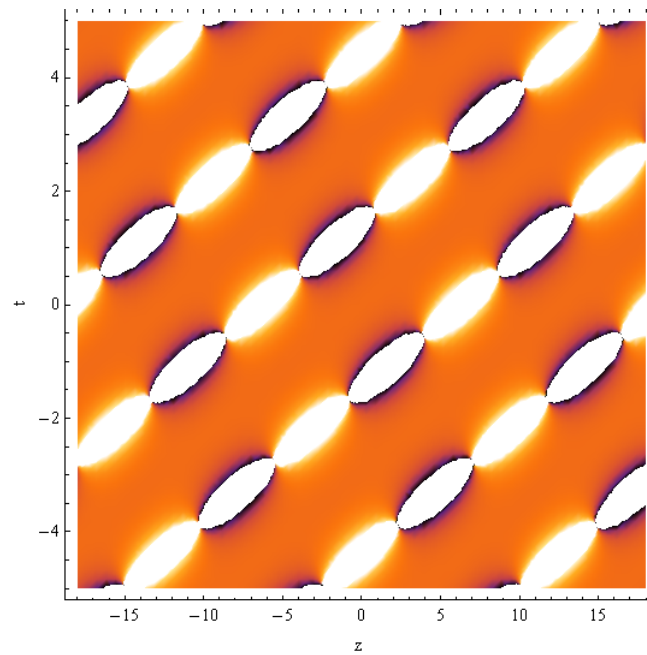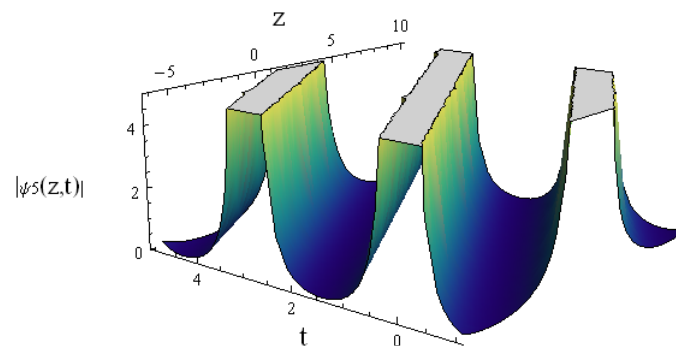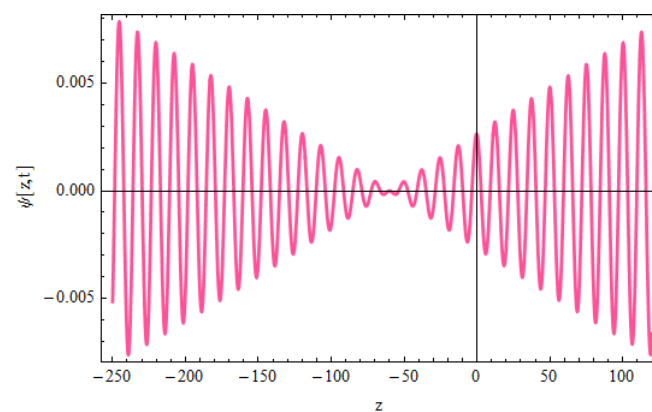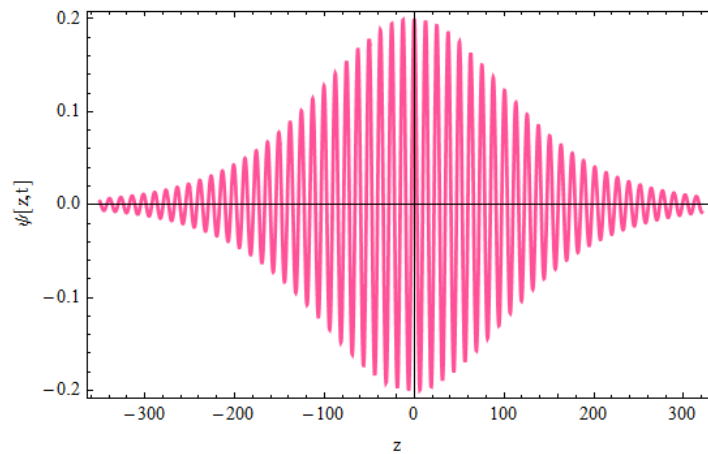**Figure 3.** Change of solution (12) with z, t for $c = 0.5$, $v = 0.7$, $\beta_1 = 0.1$, $\beta_2 = 1$, $\beta_1 = 0.1$, $\beta_3 = 0.3$, $\beta_4 = 0.2$.

Figure 4. Change of solution (14) with z, t for $c = 0.5$, $v = 0.7$, $\beta_1 = 0.1$, $\beta_2 = 1$, $\beta_1 = 0.1$, $\beta_3 = 0.3$, $\beta_4 = 0.2$.

Figure 5. Change of real part of solution (16) with z, t for $c = 0.5$, $v = 0.7$, $\beta_1 = 0.1$, $\beta_2 = 1$, $\beta_3 = 0.3$, $\beta_4 = 0.2$.
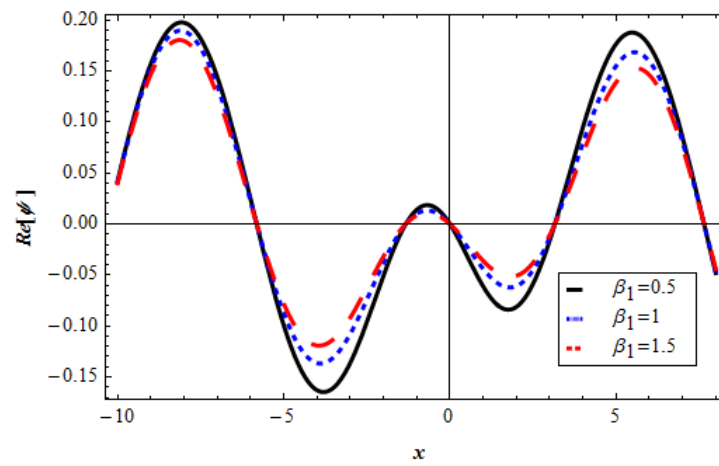

Figure 6. Change of solution (16) with z, t for $c = 0.5$, $v = 0.7$, $\beta_1 = 0.05$, $\beta_2 = 1$, $\beta_3 = 0.3$, $\beta_4 = 0.2$.

Figure 7. Change of real part of solution (19) with z, t for $c = 0.5$, $v = 0.7$, $\beta_1 = 0.05$, $\beta_2 = 1$, $\beta_3 = 0$, $\beta_4 = 0$.

Figure 8. Change of real part of solution (20) with z, t for $c = 0.5$, $v = 0.7$, $\beta_1 = 0.05$, $\beta_2 = 1$, $\beta_3 = 0, \beta_4 = 0$.

Figure 9. Change of solution (19) with z, t, β_1 for $c = 0.5$, $v = 0.7$, $\beta_2 = 1$, $\beta_3 = 0$, $\beta_4 = 0$.
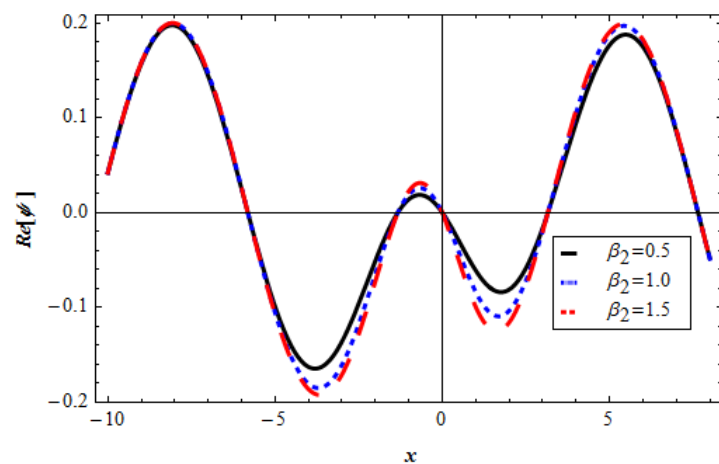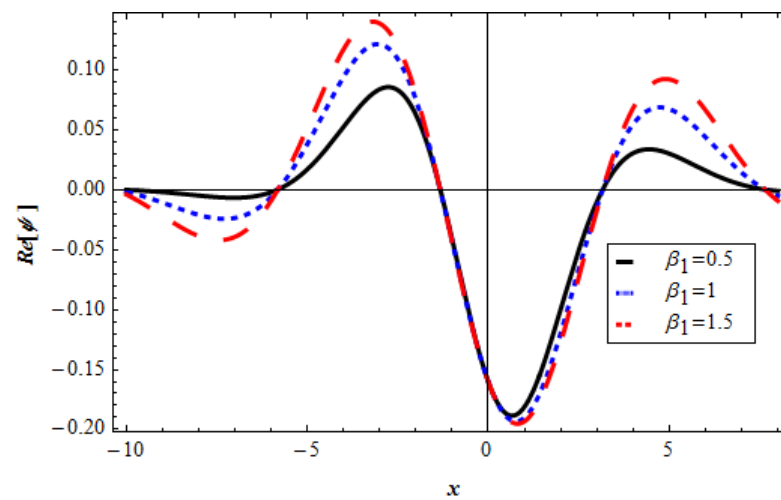

Figure 10. Change of solution (20) with z, t, β_2 for $c = 0.5$, $v = 0.7$, $\beta_1 = 0.1$, $\beta_3 = 0$, $\beta_4 = 0$.

Figure 11. Change of solution (19) with z, t, β_1 for $c = 0.5, v = 0.7, \beta_2 = 0.1, \beta_3 = 0, \beta_4 = 0$.
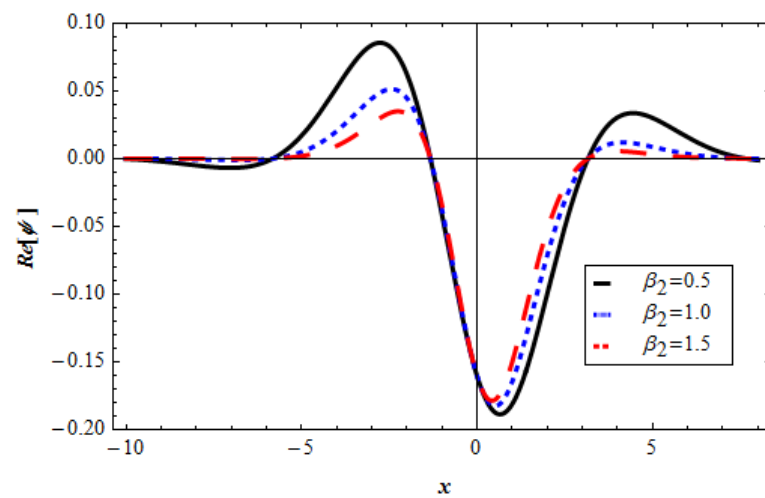

Figure 12. Change of solution (20) with z, t, β_2 for $c = 0.5, v = 0.7, \beta_1 = 0.1, \beta_3 = 0, \beta_4 = 0$.
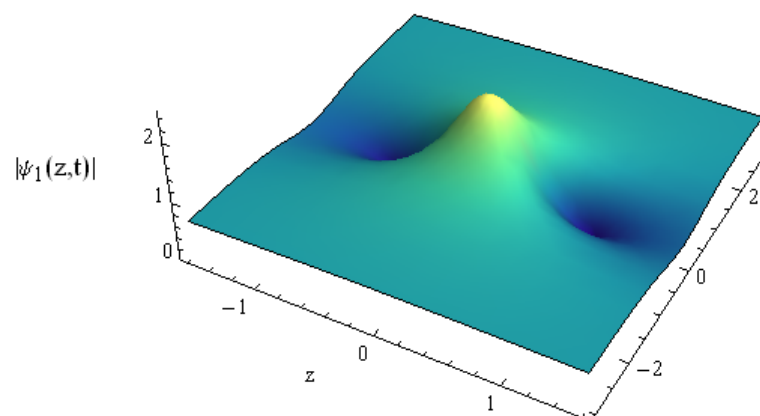

Figure 13. Change of solution (21) with z, t for $c = 0.5, v = 0.7, \beta_2 = 1, \beta_3 = 0, \beta_4 = 0$.
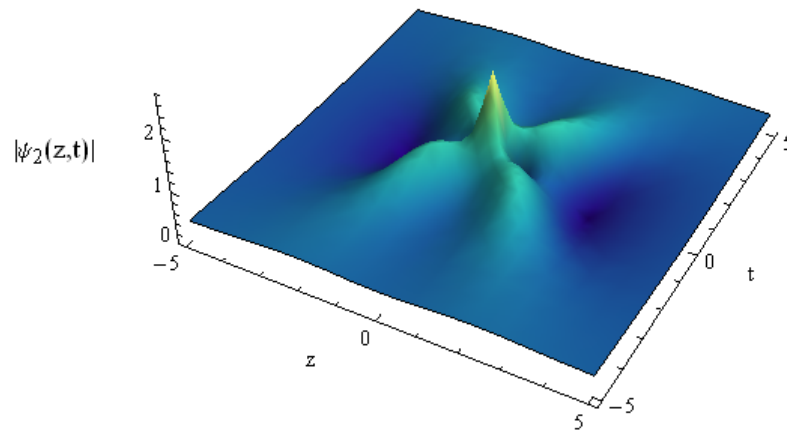
Figure 14. Change of solution (22) with z, t for $c = 0.5, v = 0.7, \beta_1 = 0.1, \beta_2 = 1, \beta_3 = 0, \beta_4 = 0$.
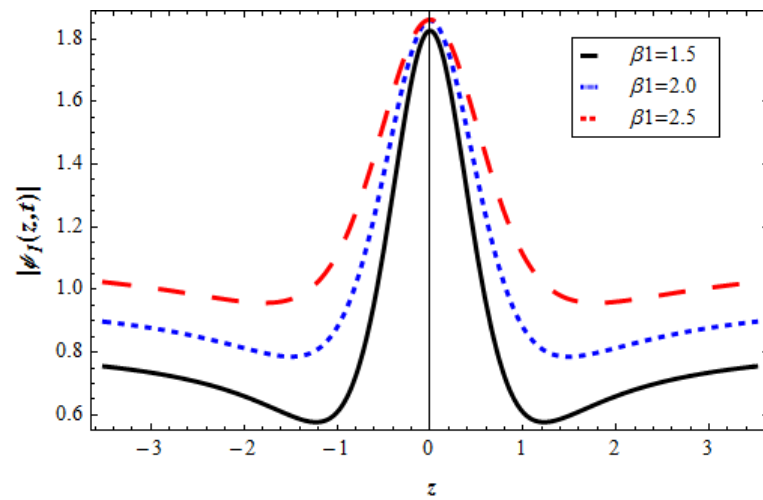

Figure 15. Change of solution (21) with z, t, β_1 for $c = 0.5, v = 0.7, \beta_2 = 1, \beta_3 = 0, \beta_4 = 0$.
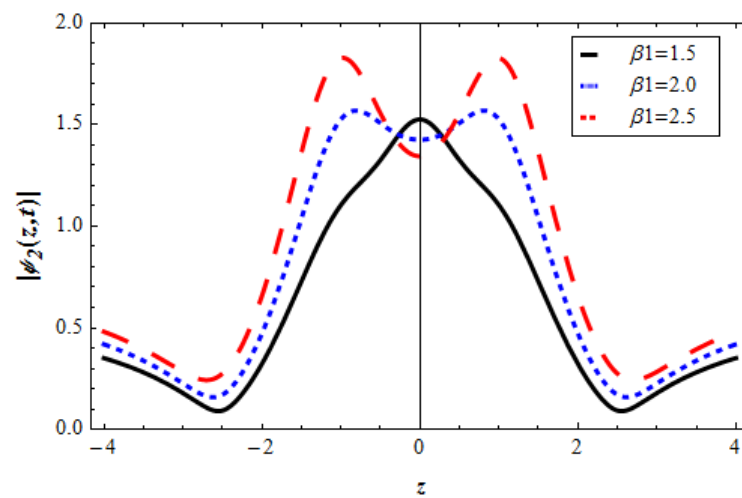

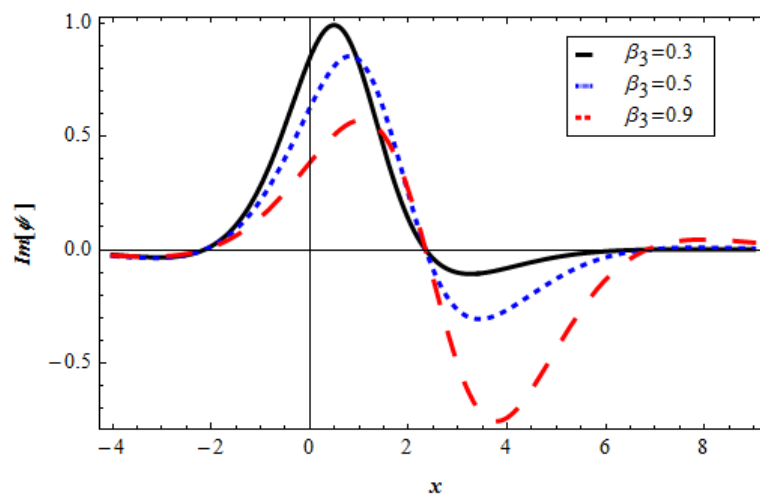**Figure 16.** Change of solution (22) with z, t, β_1 for $c = 0.5, v = 0.7, \beta_2 = 1, \beta_3 = 0, \beta_4 = 0$.

Figure 17. Change of solution (14) with z, t, β_3 for $c = 0.5, v = 0.7, \beta_1 = 0.1, \beta_2 = 1, \beta_4 = 0.2$.
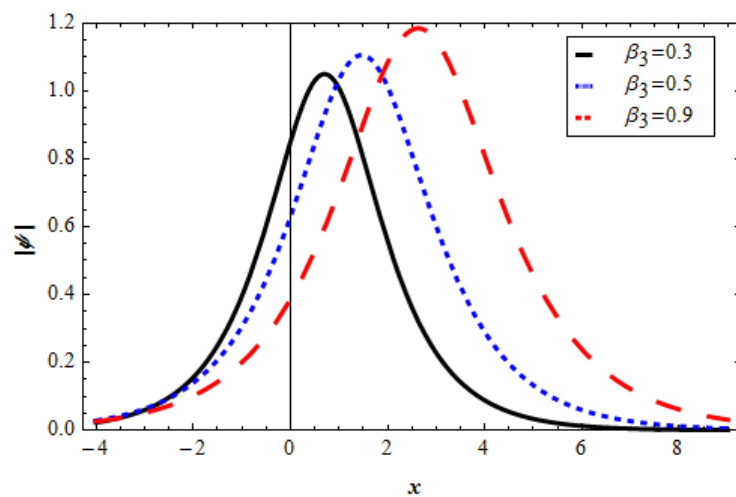

Figure 18. Change of solution (14) with z, t, β_3 for $c = 0.5, v = 0.7, \beta_1 = 0.1, \beta_2 = 1, \beta_4 = 0.2$.
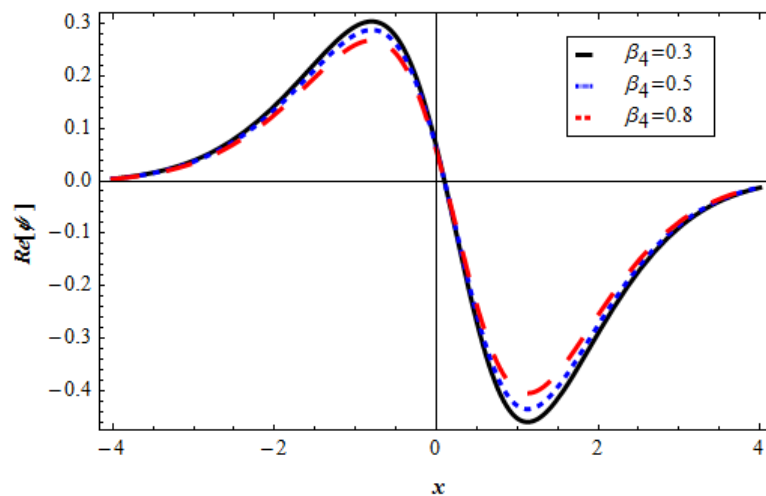

Figure 19. Change of solution (14) with z, t, β_4 for $c = 0.5, v = 0.7, \beta_1 = 0.1, \beta_2 = 1, \beta_3 = 0.3$.
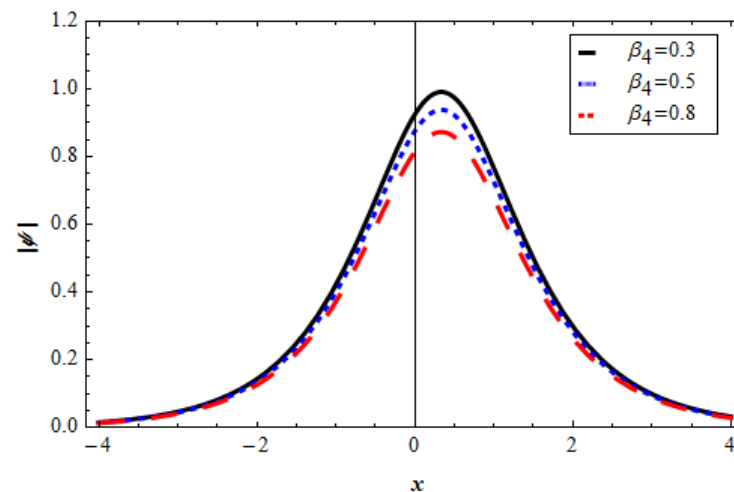
Figure 20. Change of solution (14) with z, t, β_4 for $c = 0.5, v = 0.7, \beta_1 = 0.1, \beta_2 = 1, \beta_3 = 0.3$.

4. Conclusions

In this work, the unified solver approach was used to modify resultant structures such as breather envelopes, dark, bright, huge, rational, explosive waves, and other higher-order solitary waves. In addition, the reliance on sensitivity to higher-order coefficients has been carefully considered. It was determined that higher-order coefficients impose dominance over new wave excitations such super-freak waves as well as the structure properties and energy. Additionally, a variety of significant complicated phenomena in wave energy and its applications are explained by the novel HONLSE solutions.

Author Contributions: H.G.A.: Conceptualization, Software, Formal analysis, Writing—original draft. A.F.A.: Conceptualization, Data curation, Writing—original draft. E.K.E.-S.: Conceptualization, Software, Formal analysis, Writing—original draft. M.A.E.A.: Conceptualization, Software, Formal analysis, Writing—review editing. All authors have read and agreed to the published version of the manuscript.

Institutional Review Board Statement: Not applicable.

Informed Consent Statement: Not applicable.

Data Availability Statement: Data sharing is not applicable to this article as no datasets were generated or analysed during the current study.

Conflicts of Interest: The authors declare that they have no competing interests.

Reference

1. Biondini, G.; El, G.A.; Hoefer, M.A.; Miller, P.D. Dispersive hydrodynamics: Preface. *Physica D* **2016**, *333*, 1–5. [CrossRef]
2. Chang, J.J.; Engels, P.; Hoefer, M.A. Formation of dispersive shock waves by merging and splitting Bose-Einstein condensates. *Phys. Rev. Lett.* **2008**, *101*, 170404. [CrossRef] [PubMed]
3. Dutton, Z.; Budde, M.; Slowe, C.; Hau, L.V. Observation of quantum shock waves created with ultra-vompressed slow light pulses in a Bose-Einstein condensate. *Science* **2001**, *293*, 663–668. [CrossRef] [PubMed]
4. Agrawal, G.P. *Nonlinear Fiber Optics*; Academic: San Francisco, CA, USA, 1995.
5. Triki, H.; Bensalem, C.; Biswas, A.; Khan, S.; Zhou, Q.; Adesanya, S.; Moshokoa, S.P.; Belic, M. Self-similar optical solitons with continuous-wave background in a quadratic-cubic non-centrosymmetric waveguide. *Opt. Commun.* **2019**, *437*, 392–398. [CrossRef]
6. Nakkeeran, K. Bright and dark optical solitons in fiber media with higher-order effects. *Chaos Solitons Fractals* **2002**, *13*, 673–679. [CrossRef]
7. Guan, W.Y.; Li, B.Q. New observation on the breather for a generalized nonlinear Schrödinger system with two higher-order dispersion operators in inhomogeneous optical fiber. *Optik* **2019**, *181*, 853–861. [CrossRef]
8. Yang, J. *Nonlinear Waves in Integrable and Nonintegrable Systems*; SIAM: Philadelphia, PA, USA, 2010.

9. Li, B.Q.; Ma, Y.L. Periodic and N-kink-like optical solitons for a generalized Schrödinger equation with variable coefficients in an inhomogeneous fiber system. *Optik* **2019**, *179*, 854–860. [CrossRef]

10. Alharbi, Y.F.; Abdelrahman, M.A.E.; Sohaly, M.A.; Inc, M. Stochastic treatment of the solutions for the resonant nonlinear Schrödinger equation with spatio-temporal dispersions and inter-modal using beta distribution. *Eur. Phys. J. Plus* **2020**, *135*, 368. [CrossRef]

11. Abdelwahed, H.G.; El-Shewy, E.K.; Abdelrahman, M.A.E.; Alsarhana, A.F. On the physical nonlinear (n+1)-dimensional Schrödinger equation applications. *Results Phys.* **2021**, *21*, 103798. [CrossRef]

12. Kivshar, Y.S.; Agrawal, G.P. *Optical Solitons: From Fibers to Photonic Crystals*; Academic Press: San Diego, CA, USA, 2003.

13. Abdelrahman, M.A.E.; Abdo, N.F. On the nonlinear new wave solutions in unstable dispersive environments. *Phys. Scripta* **2020**, *95*, 045220. [CrossRef]

14. Abdelwahed, H.G.; Abdelrahman, M.A.E.; Alghanim, S.; Abdo, N.F. Higher-order Kerr nonlinear and dispersion effects on fiber optics. *Results Phys.* **2021**, *26*, 104268. [CrossRef]

15. Chen, J.; Pelinovsky, D.E.; Upsal, J. Modulational instability of periodic standing waves in the derivative NLS equation. *J. Nonlinear Sci.* **2021**, *31*, 58. [CrossRef]

16. McDonald, G.D.; Kuhn, C.C.N.; Hardman, K.S.; Bennetts, S.; Everitt, P.J.; Altin, P.A.; Debs, J.E.; Close, J.D.; Robins, N.P. Bright solitonic matter-wave interferometer. *Phys. Rev. Lett.* **2014**, *113*, 013002. [CrossRef] [PubMed]

17. Ma, Y.L. Nth-order rogue wave solutions for a variable coefficient Schrödinger equation in inhomogeneous optical fibers. *Optik* **2022**, *251*, 168103. [CrossRef]

18. Li, B.Q.; Ma, Y.L. Interaction properties between rogue wave and breathers to the manakov system arising from stationary self-focusing electromagnetic systems. *Chaos Solitons Fractals* **2022**, *156*, 111832. [CrossRef]

19. Husakou, A.V.; Herrmann, J. Supercontinuum generation of higher-order solitons by fission in photonic crystal fibers. *Phys. Rev. Lett.* **2001**, *87*, 203901. [CrossRef] [PubMed]

20. Roy, S.; Bhadra, S.K.; Agrawal, G.P. Perturbation of higher-order solitons by fourth-order dispersion in optical fibers. *Opt. Commun.* **2009**, *282*, 3798–3803. [CrossRef]

21. Liu, C. Exact solutions for the higher-order nonlinear Schrödinger equation in nonlinear optical fibres. *Chaos Solitons Fractals* **2005**, *23*, 949–955. [CrossRef]

22. Tamilthiruvalluvar, R.; Wamba, E.; Subramaniyan, S.; Porsezian, K. Impact of higher-order nonlinearity on modulational instability in two-component Bose-Einstein condensates. *Phys. Rev. E* **2019**, *99*, 032202. [CrossRef]

23. Alharbi, Y.F.; Sohaly, M.A.; Abdelrahman, M.A.E. Fundamental solutions to the stochastic perturbed nonlinear Schrödinger's equation via gamma distribution. *Results Phys.* **2021**, *25*, 104249. [CrossRef]

24. Alkhidhr, H.A.; Abdelwahed, H.G.; Alghanim, M.A.E.A.S. Some solutions for a stochastic NLSE in the unstable and higher order dispersive environments. *Results Phys.* **2022**, *34*, 105242. [CrossRef]

25. Ma, Y.L. Interaction and energy transition between the breather and rogue wave for a generalized nonlinear Schrödinger system with two higher-order dispersion operators in optical fibers. *Nonlinear Dyn.* **2019**, *97*, 95–105. [CrossRef]

26. Li, B.Q. Phase transitions of breather of a nonlinear Schrödinger equation in inhomogeneous optical fiber system. *Optik* **2020**, *217*, 164670. [CrossRef]

27. Li, B.Q.; Ma, Y.L. Extended generalized Darboux transformation to hybrid rogue wave and breather solutions for a nonlinear Schrödinger equation. *Appl. Math. Comput.* **2020**, *386*, 125469. [CrossRef]

28. Whitham, G.B. *Linear and Nonlinear Waves*; Wiley: New York, NY, USA, 1974.

29. Whitham, G.B. On the propagation of weak shock waves. *J. Fluid Mech.* **1956**, *1*, 290–318. [CrossRef]

30. Musher, S.L.; Rubenchik, A.M.; Zakharov, V.E. Weak Langmuir turbulence. *Phys. Rep.* **1995**, *252*, 178–274. [CrossRef]

31. XGao, Y.; Guo, Y.J.; Shan, W.R. Optical waves/modes in a multicomponent inhomogeneous optical fiber via a three-coupled variable-coefficient nonlinear Schrödinger system. *Appl. Math. Lett.* **2021**, *120*, 107161.

32. Li, B.Q.; Ma, Y.L. N-order rogue waves and their novel colliding dynamics for a transient stimulated Raman scattering system arising from nonlinear optics. *Nonlinear Dyn.* **2020**, *101*, 2449–2461. [CrossRef]

33. Gao, X.Y.; Guoa, Y.J.; Shanb, W.R. Looking at an open sea via a generalized (2+1)-dimensional dispersive long-wave system for the shallow water: Scaling transformations, hetero-Bäcklund transformations, bilinear forms and N solitons. *Eur. Phys. J. Plus* **2021**, *136*, 893. [CrossRef]

34. Stepanyants, Y.A.; Zakharov, D.V.; Zakharov, V.E. Lump interactions with plane solitons. *Radiophys Quantum El* **2022**, *64*, 665–680. [CrossRef]

35. Kachulin, D.; Dyachenko, A.; Zakharov, V.E. Soliton turbulence in approximate and exact models for deep water waves. *Fluids* **2020**, *5*, 67. [CrossRef]

36. Dyachenko, S.A.; Nabelek, P.; Zakharov, D.V.; Zakharov, V.E. Primitive solutions of the Korteweg–de Vries equation. *Theor Math Phys.* **2020**, *202*, 334–343. [CrossRef]

37. Liu, Y.; Wang, D.S. Exotic wave patterns in Riemann problem of the high-order Jaulent-Miodek equation: Whitham modulation theory. *Stud. Appl. Math.* **2022**, *149*, 588–630. [CrossRef]

38. Cheemaa, N.; Younis, M. New and more exact traveling wave solutions to integrable (2+1)-dimensional Maccari system. *Nonlinear Dyn.* **2016**, *83*, 1395–1401. [CrossRef]

39. Alomair, R.A.; Hassan, S.Z.; Abdelrahman, M.A.E. A new structure of solutions to the coupled nonlinear Maccari's systems in plasma physics. *AIMS Math.* **2022**, *7*, 8588–8606. [CrossRef]
40. Kourakis, I.; Shukla, P.K. Exact theory for localized envelope modulated electrostatic wavepackets in space and dusty plasmas. *Nonlinear Process. Geophys.* **2005**, *12*, 407–423. [CrossRef]
41. Noman, A.A.; Islam, M.K.; Hassan, M.; Banik, S.; Chowdhury, N.A.; Mannan, A.; Mamun, A.A. Dust-ion-acoustic rogue waves in a dusty plasma having super-thermal electrons. *Gases* **2021**, *1*, 106–116. [CrossRef]
42. Akhmediev, N.; Ankiewicz, A.; Soto-Crespo, J.M. Rogue waves and rational solutions of the nonlinear Schrödinger equation. *Phys. Rev. E* **2009**, *80*, 026601. [CrossRef] [PubMed]